Journal of Engineering and Technological Sciences

Research Paper

Influence of Heat and Mechanical Treatments on the Mechanical and Structural Characteristics of Molded Manganese Steels

Omar Ben Lenda[1,2], Hajar El Ganich[3], Sara Benmaziane[2] & Elmadani Saad[2,3]

[1]The National Higher School of Mining of Rabat (ENSMR), Materials, Mining and Environment: Materials Science and Engineering, BP: 753, Agdal-Rabat, Morocco
[2]Laboratory of Physical-Chemistry of Processes and Materials, Faculty of Sciences and Technology Settat, Hassan 1st University, BP: 577, 26000 Settat, Morocco
[3]Hassan First University of Settat, High Institute of Health Sciences, Laboratory of Sciences and Engineering of Biomedicals, Biophysics and Health, B.P: 555, 26000 Settat, Morocco

*Corresponding author: benlenda@enim.ac.ma

Abstract

This paper presents a study to improve the performance of Fe-Mn-C cast steels containing 1.7% and 2.7% Cr by weight, using two treatment methods (thermal and mechanical) applied separately to two different steel grades. This approach enables an extended service life for components such as crusher liners, mill hammers, and level crossings, without requiring complete recasting. The experimental techniques used for characterization included spark optical emission spectroscopy, optical microscopy, scanning electron microscopy, as well as micro- and macro-hardness testing. Steel 1, with a composition of 15.51% Mn, 2.68% Cr, and 1.29% C, was heat-treated at 1070 °C and quenched in water, using different holding times and thicknesses. It was found that increasing the holding time from 30 to 50 minutes and reducing the thickness from 150 to 100 millimeters led to a complete and homogeneous dissolution of carbides. As a result, Steel 1 exhibited increased ductility. Steel 2 contains 13.45% Mn, 1.72% Cr, and 1.21% C. It underwent manual mechanical treatment, which resulted in surface hardening due to the transformation of austenite into martensite.

Keywords: *carbides; hardness; heat treatment; manganese steel; mechanical treatment; microstructure*.

Introduction

Manganese steel, invented by Sir Robert Hadfield in 1882, contains about 1.2% C and 12% Mn and has a face-centered cubic structure (Adler et al., (1986)). This type of steel combines high ductility and hardness with good wear resistance (Grässel et al., (2000)). Carbon promotes alloy hardening by precipitation, while manganese improves mechanical properties at elevated temperatures (Chen et al., (2010)). Austenitic manganese steel is still widely used, though often with slight compositional modifications. Scientific articles have proven that increasing the percentage of manganese to 5-10% and adjusting the percentage of carbon to 0.1-0.2% improves mechanical performance. During intercritical annealing, Luo et al. (2011) established experimental and numerical evidence showing that a high-manganse content promotes the formation of thermally stable austenite. Shi et al. (2010) found that steels with a high proportion of metastable austenite, thanks to strain-induced transformation, exhibit increased work hardening and a better balance between strength and ductility. Merwin (2007) also demonstrated that low-carbon, manganese-rich percentages lead to significant improvements in ductility and energy absorption, making these steels suitable for advanced forming processes.

Given their importance in the industrial field, steels have been the subject of extensive studies aimed at gaining a better understanding of their metallurgical behavior (Abdulqadir et al., (2024), Farida and Suratman (2023), Arifvianto et al., (2020), Pusparizkita et al., (2020), Soler et al., (2017), Ben Lenda et al., (2021), Benmaziane et al., (2022)). The mechanical properties of manganese steel are renowned for their interesting combination of hardness and ductility (Chen et al., (2020) and Niu et al., (2010)). Although not the hardest, this steel has a remarkable ability to harden when subjected to impact. Thanks to these characteristics, it is often preferred in many industrial applications. Among these

ISSN: 2337-5779
J. Eng. Technol. Sci. Vol. 58, No. 3, 2026, 299-309
DOI: 10.5614/j.eng.technol.sci.2026.58.3.1

studies is the work of S. Ayadi and A. Hadji, (2021) whose study examines the impact of chemical composition and heat treatment on the microstructure and wear resistance of manganese steels. According to their results, the rise in temperature during heat treatment favors two phenomena: martensitic transformation, on the one hand, and carbide dissolution on the other. As a result, the hardness of manganese steels increases and their wear behavior improves (Ayadi and Hadji (2021)). Further, Yıldırım et al. (2024) examined the effect of heat treatment on the microstructure, hardness and impact strength of high-manganese steels. Their research revealed that carbide solubility increases as heat treatment temperature rises, leading to a noticeable increase in toughness. However, they also observed that as the austenitizing temperature increases, the hardness decreases.This phenomenon is explained by the increase in the amount of carbides dissolved in the austenitic structure as the austenitizing temperature rises (Yıldırım et al., (2024)). Besides, in a study conducted by D. Bańkowski et al., (2024) the influence of work-hardening on the microstructure and hardness of Hadfield steel was examined. Their results indicate a clear improvement in the alloy's hardness following solution heat treatment and work hardening (Bańkowski et al., (2024)).

Manganese steels are widely used in Moroccan foundries. However, they are unsuitable for use in the as-cast state due to the presence of excess manganese and chromium carbides, which make them brittle (Agunsoye and Talabi, (2016); Vdovin et al., (2017)). In fact, the carbide precipitation at grain boundaries promotes the propagation of microcracks (Bańkowski et al., (2024)). The aim of this study is to thermally and mechanically treat these types of steel in order to obtain a steel that would be suitable for several industrial applications. Previous studies focus almost exclusively on wrought Hadfield alloys containing less than 0.5% Cr by weight, and in this paper, the Fe-Mn-C cast steels studied contain a higher chromium content (1.7 to 2.7% Cr by weight) (Allain et al., (2004), De Cooman et al., (2012), Bouaziz et al., (2011)). In our study, we focused on two types of manganese steel; the first steel is composed mainly of 15.51% Mn, 2.68% Cr, and 1.29% C, while the second steel is composed of 13.45% Mn, 1.72% Cr, and 1.21% C. For the first steel, heat treatment was carried out at an austenitizing temperature of 1070°C, followed by water quench cooling. For the second steel, a mechanical treatment was applied. Then, we characterized these steels using the following techniques: optical emission spectrometry, optical microscopy, scanning electron microscopy, as well as macro-hardness and micro-hardness tests.

Materials and methods

Alloy Elaboration

The alloys studied are manganese steels. Steel 1 consists essentially of 15.51% Mn, 2.68% Cr and 1.29% C, while Steel 2 contains 13.45% Mn, 1.72% Cr, and 1.21% C. Our alloys are produced as follows: the elements are melted in an electric arc furnace equipped with carbon electrodes at a temperature of almost 1500°C (Balogun et al., (2008)). Before casting the raw steel into molds, its chemical composition has been refined by adding various elements (manganese, chromium, silicon, copper, nickel, phosphorus, vanadium, tungsten, molybdenum, cobalt, niobium, sulfur, aluminum, and titanium) to produce the two grades.

Heat and Mechanical Treatments

We fixed the treatment temperature, time and nature of the cooling bath and then, studied the influence of the holding time in the furnace and the thickness of the specimen by comparing the structure of the steel before and after treatment. Steel 1 was heat-treated at an austenitizing temperature of 1070 °C, followed by water quenching. The parameters of the three heat treatments carried out on steel 1 are presented in Table 1.

Table 1 Heat treatment parameters of the steel 1.

	Heat treatment 1	**Heat treatment 2**	**Heat Treatment 3**
Specimen thickness (mm)	150	150	≤ 100
Treatment temperature (°C)	1070	1070	1070
Furnace holding time (min)	30	50	50
Cooling bath	Water	Water	Water
Cooling time (min)	10	10	10

The austenitizing temperature was set at 1070 °C in order to dissolve the carbides and avoid the melting range. Two holding times (30 and 50 minutes) were selected to compare partial and complete homogenization of the carbides. In order to reflect practical conditions, samples with thicknesses of 150 mm (as cast) and less than or equal to 100 mm (machined) were examined. All samples were then soaked in water for 10 minutes in order to maintain a fully austenitic matrix and prevent carbide re-precipitation. Steel 2 was clamped in a vise using a pair of pliers, then successive manual forces were applied to the surface of the specimen using a hammer at room temperature. Using a 2 kg hammer dropped

DOI: 10.5614/j.eng.technol.sci.2026.58.3.1

from a fixed height of 150 mm, an experienced operator performed ten identical blows on each sample. The protocol was repeated on three identical samples. Plastic deformation of a crystalline material modifies its properties by influencing its internal structure (Allain (2004)). These evolutions in properties and microstructure are known as work hardening.

Optical Emission Spectrometry

The spark emission spectrometer used was a JOBIN YVON METALYS. The specimens were prepared using a disc resurfacer, as they had to be flat and free of defects. Spark optical emission spectrometry was employed to determine the chemical composition of the alloys, based on the temporal analysis of the spectrum of optical radiation emitted by the sample when subjected to a high-frequency pulsed electrical discharge (Soltanpour et al., (1982)).

Optical Microscopy and Scanning Electron Microscopy

To examine the structural changes, we used optical microscopy and scanning electron microscopy on rectangular samples with dimensions of 10 × 10 × 10 mm³. For manganese steels, micrographic analysis requires chemical etching using a nitric alcoholic solution reagent (Nital 5%) consisting of 5 ml of nitric acid in 100 ml of pure ethanol. For microscopic examination, we used an OPTIKA metallograph with a high-resolution AIPTEK camera, and a PHILIPS XL30 ESEM scanning electron microscope (SEM). Steel phases were analyzed using energy-dispersive spectroscopy (EDS) combined with a SEM. The calculation of phase fractions was performed using image analysis software.

Macro-Hardness and Micro-hardness Tests

Hardness tests were effectuated on rectangular test samples measuring 25 × 25 × 10 mm³ using a universal durometer and following the Brinell method. In this method, the indenter is a 1.59 mm diameter steel ball with a load of 980 N. The Vickers micro-hardness test was performed using a Vickers HM-210/220 micro-durometer, using a diamond indenter with a square base and an apex angle between faces equal to 136°, under a load of 10 N. Each value reported corresponds to the average of 5 measurements well distributed over the flat section. The samples were prepared using abrasive paper (320, 600, 1200, and 4000 grit) rotating around a fixed axis with water lubrication to prevent any heating that could cause structural changes.

Results

Analysis of the Chemical Composition of the Manganese Steels

Analysis of the Chemical Composition of the Steel 1

The analysis of the chemical composition of steel 1, determined by spark emission spectrometer, is presented in Table 2. According to standard NF A 32-058, the chemical composition of steel 1 is similar to that of the austenitic manganese steel grade Z 120 MC 17 2-M.

Table 2 Chemical composition of steel 1.

Elements	Weight Percentage (wt%)
Iron	77.79
Manganese	15.51
Chromium	2.68
Carbon	1.29
Silicon	0.49
Copper	0.51
Nickel	0.82
Phosphorus	0.10
Vanadium	0.10
Tungsten	0.16
Molybdenum	0.09
Cobalt	0.16
Niobium	0.04
Sulfur	0.04
Aluminum	0.03
Titanium	58.30 ppm

Analysis of the Chemical Composition of the Steel 2

Spark optical emission spectrometry analysis of steel 2 revealed that it consists of the elements listed in Table 3. According to standard NF A 32-058, analysis of the composition of steel 2 closely corresponds to that of the austenitic manganese steel grade Z 120 MC 12-M.

Table 3 Chemical composition of steel 2.

Elements	Weight Percentage (wt%)
Iron	81.53
Manganese	13.45
Chromium	1.72
Carbon	1.21
Silicon	0.74
Copper	0.31
Nickel	0.51
Phosphorus	0.10
Vanadium	0.07
Tungsten	0.14
Molybdenum	0.06
Cobalt	**0.08**
Niobium	0.04
Sulfur	0.02
Aluminum	0.01
Titanium	66.26 ppm

Microscopic Study of the Manganese Steels

Microscopic Study of the Steel 1

Prior to heat treatment, steel 1 exhibits a fully austenitic structure in its as-cast condition. Microscopic examination reveals the presence of chromium and manganese carbides distributed throughout the microstructure. These carbides are finely dispersed and exhibit two types of distribution: some are located within the austenitic grains themselves (intragranular carbides), while others are preferentially situated at grain boundaries (intergranular carbides), as illustrated in Figures 1(a) and 1(b). The carbides exhibit relatively small dimensions and a uniform spatial distribution across the observed sections.

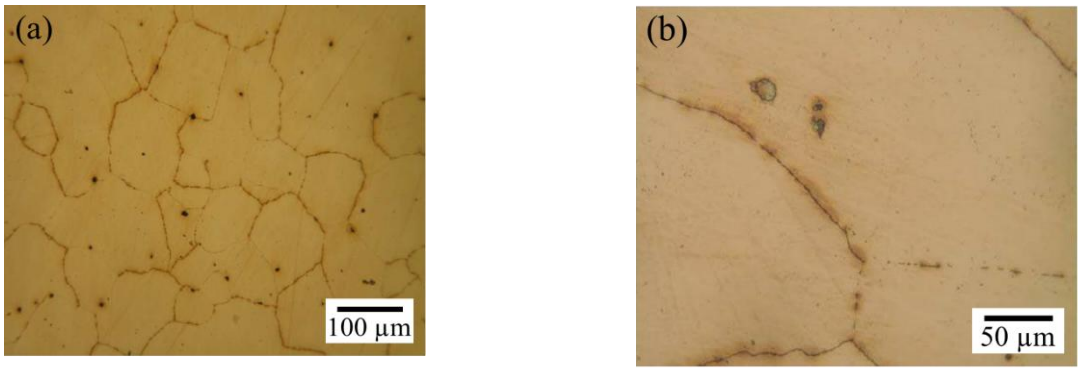

(a) (b)

Figure 1 Optical micrograph of steel 1 in the as-cast condition. Scale bars: (a) 100 µm; (b) 50 µm.

Scanning electron microscopy combined with energy-dispersive X-ray spectroscopy was employed to determine the chemical composition and thereby identify the nature of the carbide precipitates present in steel 1 in its as-cast condition (Figure 2(a)). Quantitative spectral analyses were performed using energy-dispersive X-ray spectroscopy (EDS) at two selected locations: point C3, positioned within a carbide particle, and point M2, located in the adjacent austenitic matrix. The resulting EDS spectra, presented in Figures 2(b) and 2(c) respectively, clearly indicate that the carbides in steel 1 are predominantly enriched in manganese and chromium, confirming their identity as (Cr,Mn)-rich carbides. Elemental mapping using EDS was performed to illustrate the spatial distribution of the main elements in steel 1. Figures 2d, 2e, 2f, and 2g shows the maps for iron, carbon, chromium, and manganese, demonstrating that carbon, chromium, and manganese are enriched in carbide precipitates, while iron is predominantly located in the austenitic matrix.

DOI: 10.5614/j.eng.technol.sci.2026.58.3.1

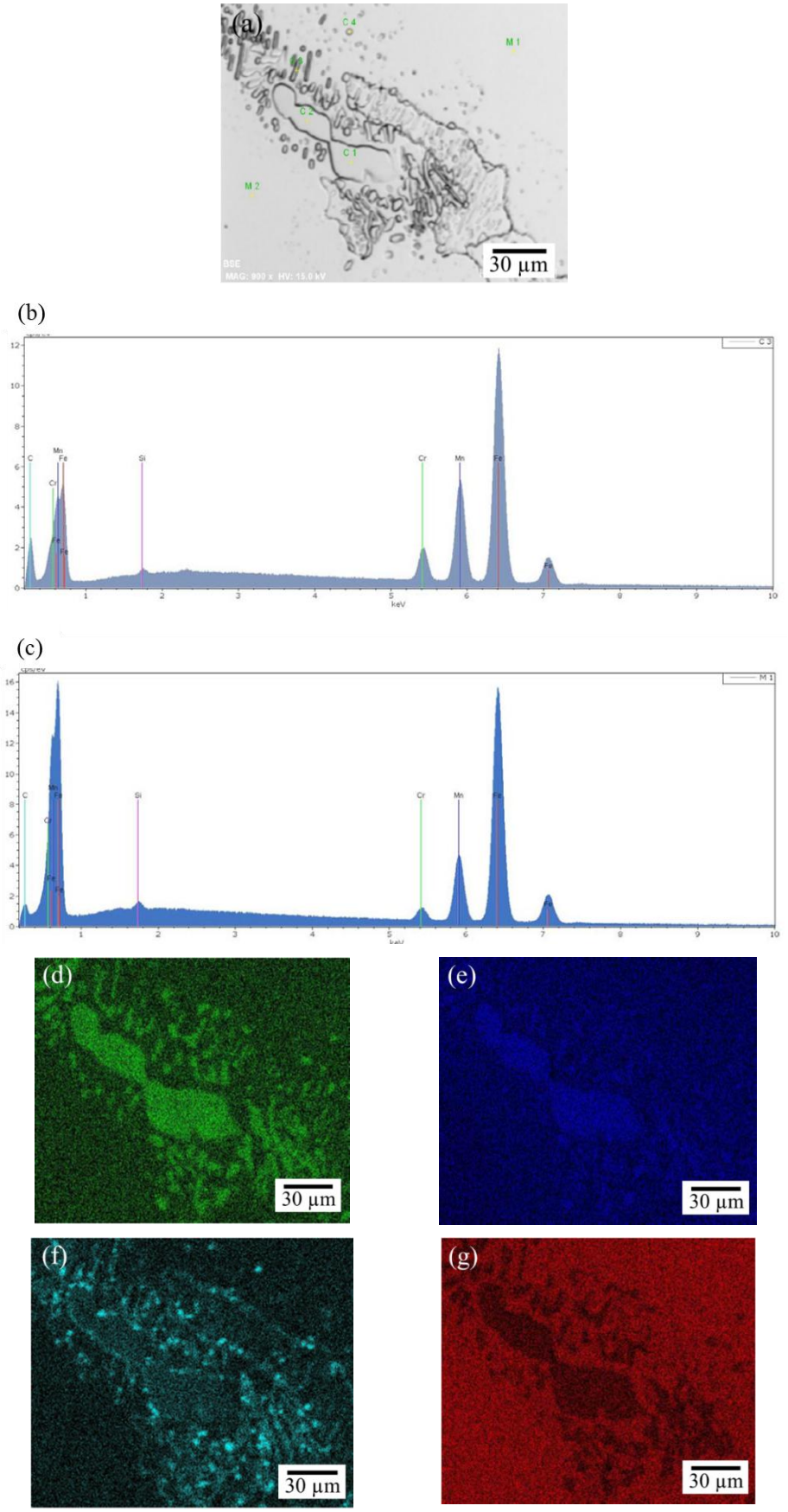

Figure 2 Microstructural and compositional characterization of steel 1 in the as-cast condition: (a) SEM image showing carbides in the austenitic matrix, (b) EDS spectrum of carbide, (c) EDS spectrum of austenitic matrix, and elemental distribution maps for (d) chromium, (e) manganese, (f) carbon, and (g) iron.

Comparative optical microscopy examination of steel 1 before (Figure 3(a) and 3(b)) and after heat treatment 1 (Figure 3(c), Figure 3(d)) reveals a slight decrease in the carbide fraction following the 30 minutes austenitizing treatment at 1070°C. However, carbide precipitates remain abundant at grain boundaries throughout the austenitic matrix. This persistence of intergranular carbides indicates that the combination of the 30 minutes holding time and the 150 mm specimen thickness was insufficient to achieve complete carbide dissolution.

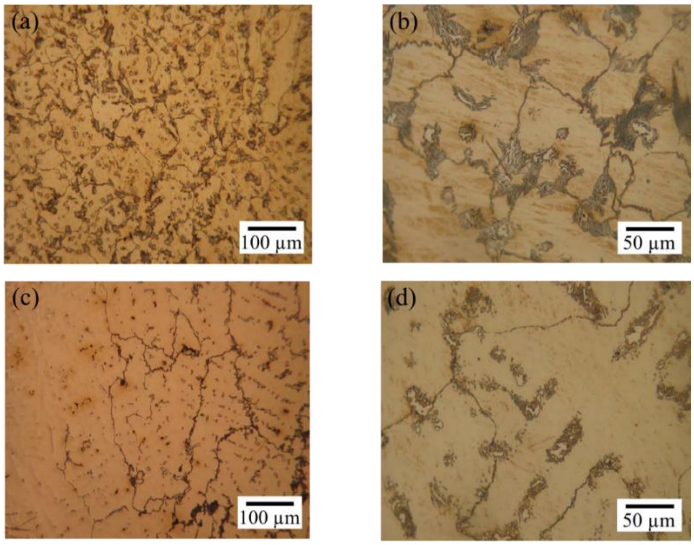

Figure 3 Optical micrographs of steel 1 before (a, b) and after (c, d) heat treatment 1.

Heat treatment 2, employing a longer holding time of 50 minutes at 1070°C, achieved partial carbide dissolution at the specimen surface (Figure 4(c), 4(d)). However, the core microstructure (Figure 4(e)) remained largely unchanged compared to the as-cast state, with excess carbide precipitates still observed at grain boundaries. This difference in carbide dissolution between surface and core is attributed to the limited thermal penetration in the 150 mm thick specimen.

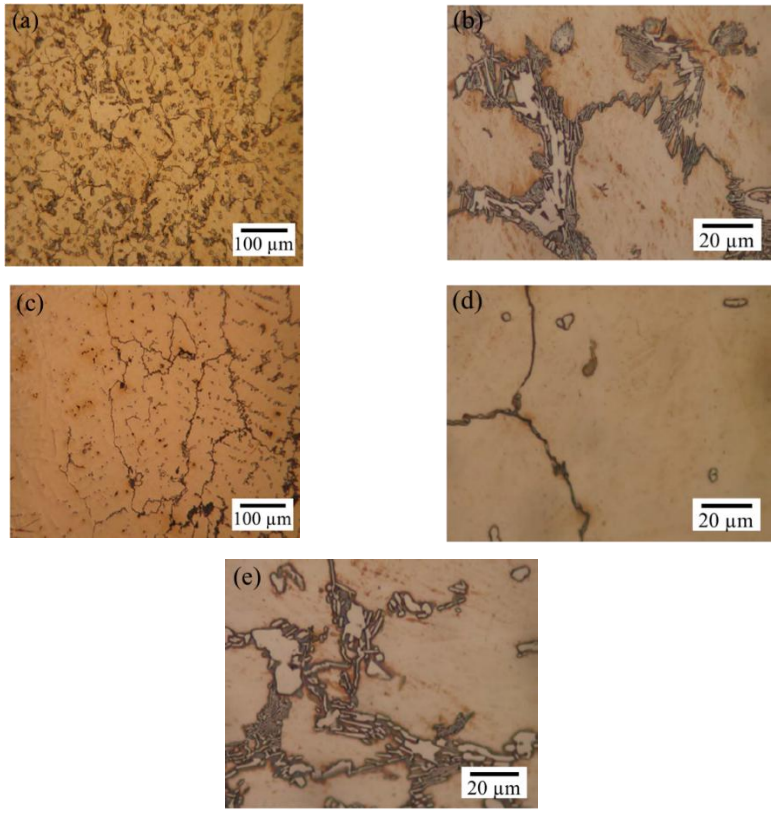

Figure 4 Optical micrographs of steel 1: (a, b) as-cast, (c, d) surface after heat treatment 2, and (e) core after heat treatment 2.

DOI: 10.5614/j.eng.technol.sci.2026.58.3.1

To evaluate the effect of specimen dimensions, heat treatment 3 used the same parameters as treatment 2 (1070°C, 50 minutes) but with reduced thickness (≤ 100 mm). Comparison of the as-cast microstructure (Figure 5(a)) with that obtained after treatment 3 (Figure 5(b)) shows that the austenitic matrix is now essentially free of carbides. Reducing the thickness decreases diffusion distances, allowing chromium and manganese to redistribute more rapidly and uniformly throughout the austenitic matrix. Additionally, the smaller cross-section ensures better thermal homogeneity, enabling uniform carbide dissolution throughout the specimen (Ismail et al., (1981)).

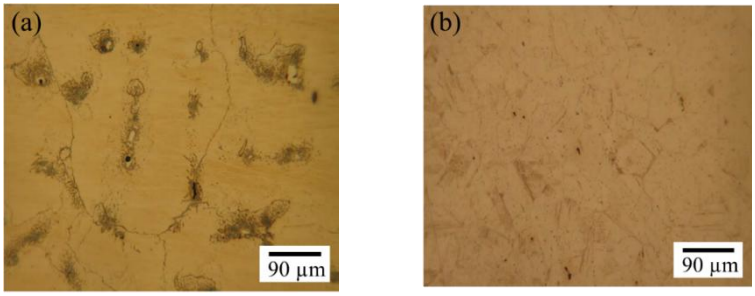

Figure 5 Optical micrographs of steel 1: (a) as-cast and (b) after heat treatment 3.

Quantitative image analysis confirms a change in the carbide fraction following heat treatment. As indicated in Table 4, the carbide fraction decreases from 6.2 ± 0.3% in the as-cast condition to 4.1 ± 0.2% after heat treatment 1. For a holding time of 50 minutes (Heat treatment 2), the carbide fraction decreased further to 1.8 ± 0.2%. Applying the same heat treatment to a thinner specimen (Heat treatment 3) led to an almost complete dissolution of the carbides.

Table 4 Fraction of carbide surface area for each heat treatment condition applied to steel 1.

Condition	Carbide area fraction (%)
As-cast	6.2 ± 0.3
Heat treatment 1	4.1 ± 0.2
Heat treatment 2	1.8 ± 0.2
Heat treatment 3	< 0.1

Micrographic Study of Steel 2

Before mechanical treatment, steel 2 exhibits an austenitic structure characterized by excess precipitates of chromium and manganese carbides located at the grain boundaries (Fig. 6). These precipitates typically form as a result of the tendency of alloying elements such as chromium and manganese to segregate at grain boundaries, where they react with carbon to form carbides. This accumulation of carbides at grain boundaries can negatively affect the steel's mechanical properties, notably its hardness and resistance to intergranular corrosion. Therefore, a thorough understanding of this initial microstructure is essential to optimize subsequent heat and mechanical treatments, in order to improve the steel's performance and long-term durability.

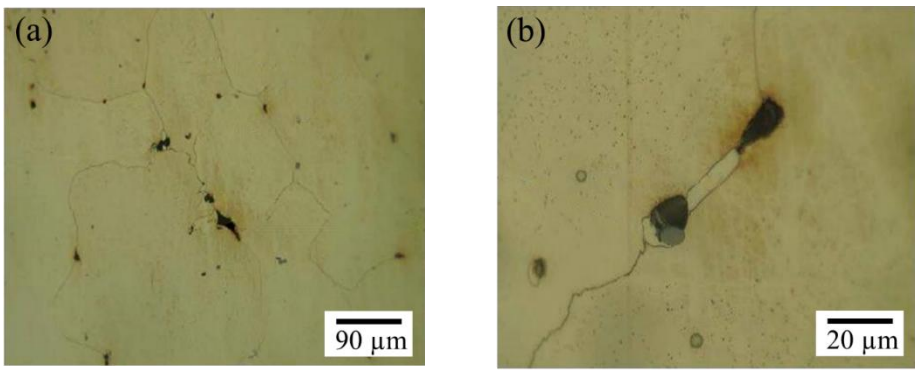

Figure 6 Optical micrograph of steel 2 in the as-cast condition. Scale bars: (a) 90 µm; (b) 20 µm.

The mechanical treatment transforms the austenitic structure of the surface of steel 2 (Figure 7(a) and 7(b)) into martensite (Figure 7(c), and 7(d)), resulting in increased surface plasticity (De Cooman (2004)). The formation of martensite is generally associated with improved hardness and strength, and in this case, it also contributes to increased surface plasticity. This improvement in plasticity can be attributed to the finer microstructure and homogeneous phase distribution resulting from the mechanical treatment, which allows the steel to absorb and distribute deformation more effectively without fracturing. As a result, mechanically treated steel 2 offers a favorable combination of hardness and plasticity, making it particularly suitable for applications requiring high wear resistance and the ability to deform without fracture under heavy loads.

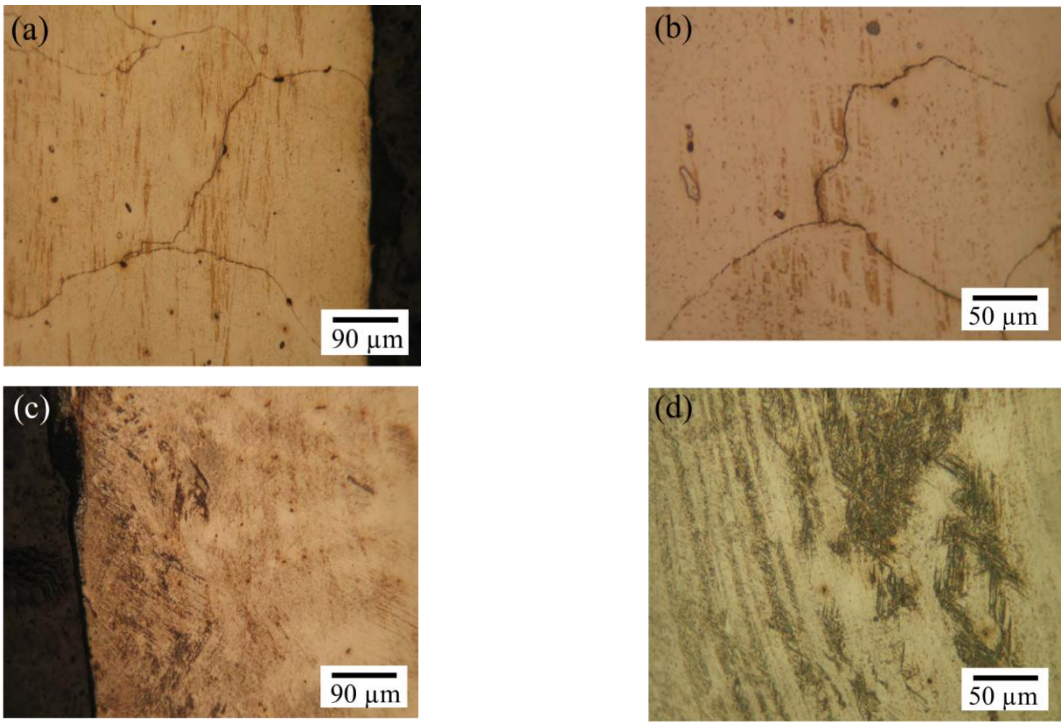

Figure 7 Optical micrographs of steel 2: (a, b) before and (c, d) after mechanical treatment.

Hardness Measurements of the Manganese Steels

Macro-hardness of the Steel 1

To quantify the microstructural changes, macro-hardness testing of steel 1 was performed before and after applying each of the three heat treatments, with measurements taken at both the core and surface (Table 5). For the surface and core of the samples, heat treatments 1 and 2 reduced the macro-hardness of steel 1 compared to its as-cast condition. The macro-hardness values measured at the core exceeded those at the surface. We conclude that increasing the holding time is necessary to ensure a uniform temperature distribution throughout the entire sample, allowing the carbides to fully dissolve across the treated volume. Following treatment 3, the macro-hardness of the specimens decreased compared with their as-cast condition, reaching a value of 190 $\pm$ 3.8 HB at the surface and 195 $\pm$ 3.6 HB at the core. After treatment 3, the macro-hardness values at both the surface and the core are almost equal, which is explained by the complete and homogeneous dispersion of the carbides in the steel 1. It can be observed that the smaller the volume to be treated, the more the carbides will dissolve, as we can easily achieve temperature uniformity in our sample.

Table 5 Core and surface macro-hardness of steel 1 before and after heat treatments.

	Surface hardness (HB)	Core hardness (HB)
Before heat treatment	270 ± 5.2	262 ± 4.8
After heat treatment 1	238 ± 4.5	249 ± 3.9
After heat treatment 2	201 ± 4.2	236 ± 3.7
After heat treatment 3	190 ± 3.8	195 ± 3.6

DOI: 10.5614/j.eng.technol.sci.2026.58.3.1

Micro-hardness of Steel 2

Table 6 presents the core and surface micro-hardness of steel 2 after mechanical treatment. Before treatment, the micro-hardness of manganese steels is relatively low, with values of 230 ± 5.4 HV at the surface and 253 ± 4.9 HV at the core of Steel 2. The mechanical treatment increased the surface micro-hardness of the specimen to 540 ± 6.3 HV, primarily due to the formation of the martensitic phase. While no change is observed in the core, which retains its initial hardness of approximately 262.4 ± 5.1 HV. This confirms that the core structure remains austenitic, with chromium carbide precipitates within the grains, similar to the microstructure of the as-cast steel.

Table 6 Micro hardness at the core and surface of steel 2 after mechanical treatment.

	Micro-hardness on surface (HV)	Micro-hardness at core (HV)
Micro-hardness after treatment	540 ± 6.3	262.4 ± 5.1

Discussion

The hardness decrease observed after solution treatment and quenching is consistent with previous findings on Hadfield-type steels. For the Hadfield grade containing 1.2% C and 12% Mn without alloying additions, the heat treatment sequence of solution treatment at 1050°C for 45 minutes followed by quenching significantly reduces the overall hardness from approximately 260 HB to around 200 HB (Ayadi, S., & Hadji, A. (2021)). These results are attributed to the almost complete dissolution of chromium- and manganese-rich carbides. Treatment 3 yields a final hardness of 195 ± 3.6 HB, which can be similarly explained by the full dissolution of chromium- and manganese-rich carbides. Yıldırım et al. (2023) observed that doubling the quenching time at a temperature of 1100 °C leads to a decrease of approximately 25 HB in overall hardness, highlighting the role of elemental diffusion in the softening of high-manganese steels (Yıldırım et al. (2024)). In our study, extending the holding time from 30 to 50 minutes also reduced hardness, which decreased from 238 ± 4.5 HB to 201 ± 4.2 HB, indicating that diffusion-controlled softening is also the determining mechanism in our material.

The significant increase in surface hardness observed in Steel 2 after mechanical treatment can be explained by the deformation behavior of austenitic manganese steels. These steels have moderate initial hardness, but undergo significant hardening even under low strain levels, resulting in high resistance to friction (Detrez (1977), Michalon et al., (1976)). Mechanical properties are improved by two mechanisms: martensite formation and the appearance of dislocations around new martensite regions due to volume expansion during the transformation of austenite into martensite (Bellhouse and McDermid (2010), Jacques et al., (2001)). The strain-induced martensitic transformation (TRIP), assisted by mechanical twinning (TWIP), accommodates shear strain, elevates dislocation density, and sustains a high work-hardening rate, allowing an increase in surface hardness to 540 ± 6.3 HV without compromising the ductility of the austenitic core (Allain et al., (2004), Jacques et al., (2001), Bouaziz et al., (2011), Bellhouse et al. (2010)).

Conclusions

This study examines two distinct treatment methods for improving Fe–Mn–C cast steels containing 1.7 wt.% and 2.7 wt.% Cr. The proposed approaches provide a practical and cost-effective means of extending the service life of industrial components operating under severe loading conditions, mechanical stresses, without requiring complete recasting or alloy modification.

Initially, both steel grades exhibited brittleness due to the formation of intergranular carbides enriched in manganese and chromium. To address this limitation, three hyper-quenching treatments at 1070 °C were applied to Steel 1. Increasing the holding time from 30 to 50 minutes led to partial dissolution of surface carbides, while further reducing the section thickness from 150 mm to 100 mm achieved complete and homogeneous dissolution throughout the sample. This process resulted in a refined and uniform microstructure, enhancing ductility and overall structural integrity. For Steel 2, a mechanical surface treatment induced a localized transformation of the surface layer from austenite to martensite. This phase transformation significantly increased surface hardness from 230 ± 5.4 HV to 540 ± 6.3 HV, while maintaining a tough austenitic core.

Overall, the results confirm that combining controlled heat treatment and mechanical treatments leads to substantial improvements in mechanical performance and structural integrity, while providing an effective means to finely adjust the hardness–toughness balance in Fe–Mn–C cast steels. Such an approach offers a reliable and economical pathway to enhance the mechanical reliability and operational lifetime of critical steel components in mining, construction, and

heavy machinery applications. In addition, these findings highlight the potential of such treatments as practical and economical alternatives for enhancing the durability and service performance of high-stress industrial components.

Compliance with ethics guidelines

The authors declare they have no conflict of interest or financial conflicts to disclose.

This article contains no studies with human or animal subjects performed by the authors.

References

Abdulqadir, S. F., Alaseel, B. H., & Sameer, J. O. (2024). Comparison of the Mechanical Properties and Approach to Numerical Modeling of Fiber-reinforced Composite, High-Strength Steel and Aluminum. *Journal of Engineering and Technological Sciences, 56*(1), 110-124.

Adler, P. H., Olson, G. B., & Owen, W. S. (1986). Strain hardening of Hadfield manganese steel. *Metallurgical and Materials Transactions A, 17,* 1725–1737.

Agunsoye, J. O., & Talabi, S. I. (2016). Properties optimization of hadfield austenitic manganese steel casting. *Ann. Fac. Eng. Hunedoara-International J. Eng.,13*(4), 101–106.

Allain, S., Chateau, J.-P., Bouaziz, O., Migot, S. & Guelton, N. (2004). Correlations between the calculated stacking-fault energy and the plasticity mechanisms in Fe–Mn–C alloys. *Materials Science and Engineering A, 387-389,* 158–162. https://doi.org/10.1016/j.msea.2004.01.059

Allain, S. (2004). Caractérisation et modélisation thermomécaniques multi-échelles des mécanismes de déformation et d'écrouissage d'aciers austénitiques à haute teneur en manganèse: application à l'effet TWIP (Doctoral dissertation, Institut National Polytechnique de Lorraine).

Arifvianto, B., Mahardika, M., & Salim, U. A. (2020). Comparison of Surface Characteristics of Medical-grade 316L Stainless Steel Processed by Sand-blasting, Slag Ballblasting and Shot-blasting Tre. *Journal of Engineering & Technological Sciences, 52(*1), 1–13.

Ayadi, S., & Hadji, A. (2021). Effect of chemical composition and heat treatments on the microstructure and wear behavior of manganese steel. *International Journal of Metalcasting, 15*(2), 510–519. https://doi.org/10.1007/s40962-020-00479-2

Balogun, S. A., Esezobor, D. E., & Agunsoye, J. O. (2008). Effect of melting temperature on the wear characteristics of austenitic manganese steel. *Journal of Minerals and Materials Characterization and Engineering, 7*(3), 277–289.

Bańkowski, D., Młynarczyk, P. S., Depczyński, W. P., & Bolanowski, K. (2024). The effect of work hardening on the structure and hardness of hadfield steel. *Archives of Foundry Engineering, 24*(1), 14–20.

Ben Lenda, O., S. Benmaziane, A. Tara, and E. Saad. (2021). Mechanical properties and microstructure evolution of high-manganese (0.9 C - 13.95 Mn) steel during aging. *E3S Web of Conferences, 297*, 01044. EDP Sciences.

Bellhouse, E. M., & McDermid, J. R. (2010). Effect of continuous galvanizing heat treatments on the microstructure and mechanical properties of high Al-low Si transformation induced plasticity steels. *Metallurgical and Materials Transactions A, 41*, 1460–1473. https://doi.org/10.1007/s11661-010-0185-7

Benmaziane, S., Ben Lenda, B., Saissi, S., Zerrouk, L., & Saad, E. (2022). Modeling of Austenite Grain Growth Behavior for AISI 302 Stainless Steel. *Recent Patents on Mechanical Engineering, 15*(5), 486–493.

Bouaziz, O., Allain, S., Scott, C., Cugy, P. & Barbier, D. High-manganese austenitic twinning-induced plasticity steels: A review of the microstructure–properties relationships. *Current Opinion in Solid State and Materials Science, 15* (4), 141–168 (2011). https://doi.org/10.1016/j.cossms.2011.04.002

Chen, M. S., Cheng, H. C., Huang, C. F., Chao, C. Y., Ou, K. L., & Yu, C. H. (2010). Effects of C and Cr content on high-temperature microstructures of Fe–9Al–30Mn–xC–yCr alloys. *Materials characterization, 61*(2), 206–211.

Chen, J., Zhang, Y., Wang, J. J., Liu, C. M., & Zhao, S. X. (2020). Multistage serrated flow behavior of a medium-manganese high-carbon steel. *Journal of Iron and Steel Research International, 27*, 1064–1072.

De Cooman, B.C., Kwon, O. & Chin, K.-G. State-of-the-knowledge on TWIP steel. *Materials Science and Technology, 28* (5), 513–527 (2012). https://doi.org/10.1179/1743284711Y.0000000095

De Cooman, B. C. (2004). Structure–properties relationship in TRIP steels containing carbide-free bainite. *Current Opinion in Solid State and Materials Science, 8*(3-4), 285-303.

Detrez, P. (1977). L'acier moulé austénitique au manganèse. *Matériaux & Techniques, 65*, 27–32.

Farida, I., & Suratman, R. (2023). The Material Science Behind Repetitive Hammering, Solution Annealing, and Tempering on Hadfield Steel. *Journal of Engineering & Technological Sciences, 55*(4), 393–401.

Grässel, O., Krüger, L., G. Frommeyer, and L. W. Meyer. (2000). High strength Fe–Mn–(Al, Si) TRIP/TWIP steels development properties application. *Int. J. Plast ,16*(10–11),1391–1409.

Ismail, M. I., Iskander, S. S., & Saleh, E. B. (1981). Carburizing of steels. *Surface Technology, 12*(4), 341–349.

DOI: 10.5614/j.eng.technol.sci.2026.58.3.1

Jacques, P., Furnémont, Q., Mertens, A., & Delannay, F. (2001). On the sources of work hardening in multiphase steels assisted by transformation-induced plasticity. *Philosophical Magazine A, 81*(7), 1789–1812.

Jacques, P.J., Delannay, F. & Ladrière, J. On the influence of interactions between phases on the mechanical stability of retained austenite in transformation-induced plasticity multiphase steels. *Metallurgical and Materials Transactions A, 32* (11), 2759–2768 (2001). https://doi.org/10.1007/s11661-001-1027-4

Luo, H., Shi, J., Wang, C., Cao, W., Sun, X., & Dong, H. (2011). Experimental and numerical analysis on formation of stable austenite during the intercritical annealing of 5Mn steel. *Acta Materialia, 59*(10), 4002–4014.

Merwin, M. (2007, February). Low-carbon manganese TRIP steels. *Materials science forum, 539*, 4327–4332. Trans Tech Publications Ltd.

Michalon, D., Mazet, G., & Burgio, C. (1976). Mise au point d'un procédé de conditionnement des aciers au manganèse pour résoudre les problèmes d'usure en présence d'abrasif. *Revue de métallurgie, 73*(10), 711–717.

Niu, L., Hojamberdiev, M., Xu, Y., & Wu, H. (2010). Microstructure and mechanical properties of Hadfield steel matrix composite reinforced with oriented high-chromium cast iron bars. *Journal of Materials Science, 45*, 4532–4538.

Pusparizkita, Y. M., Schmahl, W. W., Setiadi, T., Ilsemann, B., Reich, M., Devianto, H., & Harimawan, A. (2020). Evaluation of Bio-Corrosion on Carbon Steel by Bacillus Megaterium in Biodiesel and Diesel Oil Mixture. *Journal of Engineering & Technological Sciences, 52*(3), 370–384.

Shi, J., Sun, X., Wang, M., Hui, W., Dong, H., & Cao, W. (2010). Enhanced work-hardening behavior and mechanical properties in ultrafine-grained steels with large-fractioned metastable austenite. *Scripta Materialia, 63*(8), 815–818.

Soler, Y. I., & Nguyen, V. C. (2017). Study of Micro-hardness of High-Speed W9Mo4Co8 Steel Plates in Pendulum Grinding by Abrasive Wheel Periphery. *Journal of Engineering & Technological Sciences, 49*(3), 291–307.

Soltanpour, P. N., Jones Jr, J. B. and Workman, S. M. (1982). Optical emission spectrometry, *Methods Soil Anal. Part 2 Chem. Microbiol. Prop., 9*, 29–65.

Vdovin, K. N., Feoktistov, N. A., Gorlenko, D. A., Chernov, V. P., & Khrenov, I. B. (2017). Influence of alloying and heat treatment on the abrasive and impact–abrasive wear resistance of high-manganese steel. *Steel in Translation, 47*, 705–709.

Yıldırım, H., Erdin, M. E., & Özgedik, A. (2024). Effects of Heat Treatment on Microstructure and Impact Resistance of High Manganese Steels. *Politeknik Dergisi, 27*(5), 1805–1812. https://doi.org/10.2339/politeknik.1363853

Manuscript Received: 7 November 2024
1st Manuscript Revision Received: 8 July 2025
2nd Manuscript Revision Received: 10 September 2025
3rd Manuscript Revision Received: 13 November 2025
Accepted Manuscript: 27 November 2025